UC Irvine
UC Irvine Previously Published Works

Title

Whole-Genome Analysis Reveals that Mutations in Inositol Polyphosphate Phosphatase-like 1 Cause Opsismodysplasia

Permalink

https://escholarship.org/uc/item/0m17r3zz

Journal

American Journal of Human Genetics, 92(1)

ISSN

0002-9297

Authors

Below, Jennifer E
Earl, Dawn L
Shively, Kathryn M
et al.

Publication Date

2013

DOI

10.1016/j.ajhg.2012.11.011

Copyright Information

Peer reviewed

Whole-Genome Analysis Reveals that Mutations in Inositol Polyphosphate Phosphatase-like 1 Cause Opsismodysplasia

Jennifer E. Below,[1] Dawn L. Earl,[2,3] Kathryn M. Shively,[3] Margaret J. McMillin,[3] Joshua D. Smith,[1] Emily H. Turner,[1] Mark J. Stephan,[4] Lihadh I. Al-Gazali,[5] Jozef L. Hertecant,[5] David Chitayat,[6] Sheila Unger,[7] Daniel H. Cohn,[8,9] Deborah Krakow,[9,10] James M. Swanson,[11] Elaine M. Faustman,[12] Jay Shendure,[1] Deborah A. Nickerson,[1] Michael J. Bamshad,[1,2,3,*] and University of Washington Center for Mendelian Genomics

Opsismodysplasia is a rare, autosomal-recessive skeletal dysplasia characterized by short stature, characteristic facial features, and in some cases severe renal phosphate wasting. We used linkage analysis and whole-genome sequencing of a consanguineous trio to discover that mutations in inositol polyphosphate phosphatase-like 1 (*INPPL1*) cause opsismodysplasia with or without renal phosphate wasting. Evaluation of 12 families with opsismodysplasia revealed that *INPPL1* mutations explain ~60% of cases overall, including both of the families in our cohort with more than one affected child and 50% of the simplex cases.

Opsismodysplasia (MIM 258480) is a rare skeletal dysplasia with delayed bone maturation (from "opsismos," Greek for "late").[1–3] The clinical signs observed at birth include short limbs, small hands and feet, relative macrocephaly with a large anterior fontanel, and characteristic craniofacial abnormalities including a prominent brow, depressed nasal bridge, a small anteverted nose, and a relatively long philtrum. Death secondary to respiratory failure during the first few years of life was reported in the cases originally described but the outcome is now known to be highly variable with multiple long-term survivors.[3] Typical radiographic findings include shortened long bones with very delayed epiphyseal ossification, severe platyspondyly, metaphyseal cupping, and characteristic abnormalities of the metacarpals and phalanges. Recurrence within sibships and incidence in consanguineous pedigrees suggest that the mode of inheritance of opsismodysplasia is autosomal recessive.[1–6]

To determine the genetic basis of opsismodysplasia, one of two siblings with opsismodysplasia and severe hypophosphatemia because of renal phosphate wasting (AII-1 in Table 1, Figures 1 and 2, and Figure S1 available online) and his consanguineous parents were genotyped with the HumanCytoSNP-12 DNA Analysis BeadChip, at nearly 300,000 single-nucleotide polymorphisms (SNPs). All studies were approved by the institutional review boards of the University of Washington and Seattle Children's Hospital and informed consent was obtained from partici-

pants or their parents. Self-reported Hispanic and Native American ancestry was first confirmed with EIGENSTRAT. Parametric linkage analysis by a fully penetrant rare recessive model ($f_2 = 1$; $q = 0.0001$) and allele frequencies estimated from unrelated members of the HapMap CEPH, European, Chinese, Japanese, and Mexican American populations (Figure S2) was performed with ALLEGRO on an approximately 0.2 cM SNP map in an 11 person pedigree that included the consanguineous parents of the proband. Ten genomic regions reached a maximum LOD score of 1.5 (Figure S3). Homozygosity mapping via PLINK and default parameters (length = 1 Mb, # SNPs [n] = 100, density [kb/SNP] = 50, largest gap [kb] = 1 Mb) detected six of the regions also implicated via linkage analysis.

Next, whole-genome sequencing was performed on both parents and the same affected sibling used in the linkage studies. In brief, 1 μg of genomic DNA was subjected to a series of shotgun library construction steps, including fragmentation through acoustic sonication (Covaris), end-polishing (NEBNext End Repair kit), A-tailing (NEBNext dA Tailing kit), and ligation of 8 bp barcoded sequencing adaptors (Enzymatics Ultrapure T4 Ligase). Libraries were automatically size selected for fragments 350–550 bp in length with the automated PippinPrep cartridge system, which provides for fine control over the insert size and physically isolates each size fraction in separate chambers. Prior to sequencing, the library was amplified via PCR (Kapa HiFi Hotsart). To facilitate optimal

[1]Department of Genome Sciences, University of Washington, Seattle, WA 98195, USA; [2]Division of Genetic Medicine, Seattle Children's Hospital, Seattle, WA 98105, USA; [3]Department of Pediatrics, University of Washington, Seattle, WA 98195, USA; [4]Department of Pediatrics, Madigan Army Medical Center, Tacoma, WA 98431, USA; [5]Department of Pediatrics, United Arab Emirates University, PO Box 17666, Al Ain, United Arab Emirates; [6]Department of Obstetrics and Gynecology, The Prenatal Diagnosis and Medical Genetics Program, Mount Sinai Hospital, University of Toronto, Toronto, ON M5G 1Z5, Canada; [7]Department of Genetics, University of Lausanne, Centre Hospitalier Universitaire Vaudois, 1011 Lausanne, Switzerland; [8]Department of Molecular, Cell and Developmental Biology, University of California, Los Angeles, Los Angeles, CA 90095, USA; [9]Department of Orthopaedic Surgery, University of California, Los Angeles, Los Angeles, CA 90095, USA; [10]Department of Human Genetics, University of California, Los Angeles, Los Angeles, CA 90095, USA; [11]Department of Pediatrics, University of California, Irvine, Irvine, CA 92697, USA; [12]Department of Environmental and Occupational Health Sciences, University of Washington, Seattle, WA 98195, USA
*Correspondence: mbamshad@uw.edu

Table 1. Mutations and Clinical Findings of Individuals with Opsismodysplasia

Case identifier	AII-1	AII-2	BII-1	CII-1	DII-1		EII-1	FII-1		FII-2		GII-2
Mutations												
Exon (INNPL1)	17	17	7	7	intron 21	1	14	5	1	6	1	6	18
Nucleotide	c.1976C>T	c.1976C>T	c.768_769del	c.768_769del	c.2415+1G>A	c.35dup	c.1687_1691del	c.545C>A	c.24_39del	c.753G>C	c.24_39del	c.753G>C	c.2071C>T
Peptide	p.Pro659Leu	p.Pro659Leu	p.Glu258Alafs*45	p.Glu258Alafs*45	NA	p.Ala13Argfs*62	p.Thr563Glyfs*3	p.Ser182*	p.Gly9Trpfs*13	p.Gln251His	p.Gly9Trpfs*13	p.Gln251His	p.Arg691Trp
GERP score	5.43	5.43	NA	NA	5.52	NA	NA	NA	NA	4.77	NA	4.77	3.7
Predicted effect	missense	missense	frameshift	frameshift	splice site	frameshift	frameshift	nonsense	frameshift	missense	frameshift	missense	missense
Genotype	homozygous	homozygous	homozygous	heterozygous	heterozygous	heterozygous	heterozygous	homozygous	heterozygous	heterozygous	heterozygous	heterozygous	homozygous
Inheritance	maternal/paternal	maternal/paternal	maternal/paternal DNA unavailable	maternal	paternal	NA	NA	NA	maternal	paternal	maternal	paternal	maternal/paternal
Clinical Findings												
Ancestry	Hispanic/Native American	Hispanic/Native American	European American	European American	ND		Middle Eastern	African American/European American		African American/European American		Middle Eastern
Consanguineous parents	1st cousins once removed	1st cousins once removed	no	no	no		1st cousins	no		no		1st cousins
Prenatal findings	none	none	short limbs (3rd trimester)	short limbs at 26 weeks EGA, polyhydramnios	short limbs at 18–20 weeks EGA		oligohydram-nios	none		short limbs at 20 weeks		short limbs at 18.3 weeks, severe micromelia, and bell-shaped thorax at 22 weeks
Birth length	ND	46.5 cm	43.8 cm	45.7 cm	43 cm		49 cm	43.1 cm		47 cm		NA
Birth weight	3,380 g	3,192 g	3,120 g	3,572 g	2,745 g		3,015 g	3,100 g		3,500 g		NA
Birth OFC	ND	35.6 cm	38.5 cm (2 months)	ND	35.5 cm		35 cm	ND		36.8 cm		NA
Age at last evaluation	8 years 8 months	2 years 9 months	19 months	16 months	birth (34–35 weeks gestation)		3 years	24 years		18 years		NA
Macrocephaly	–	+ (mild)	relative	relative	relative		–	–		–		–
Large fontanel(s)	+	+	+	ND	ND		+	+		+		+
Prominent forehead	+	+ (mild)	+	+	–		–	+		+		+
Tall forehead	+	–	+	+	–		+	+		+		+
Hypertelorism	+	–	–	+	ND		+	+		+		+

Table 1.   Continued

Case identifier	AII-1	AII-2	BII-1	CII-1	DII-1	EII-1	FII-1	FII-2	GII-2
Long palpebral fissures	+	–	–	ND	ND	+	90%	–	NA
Proptosis/shallow orbits	+	–	+	+	ND	+	+	+	+
Depressed nasal root	+	+	+	ND	+	+	+	+	+ (absent nasal bone)
Short nose	+	+	+	+	+	+	+	+	+
Abnormal ears	–	–	+	ND	+ (low set)	+	posteriorly rotated, upturned lobules	–	–
Respiratory insufficiency	+ (ventilator dependent)	+ (mild to moderate)	respiratory distress	recurrent pneumonia, pulmonary hypertension, restrictive lung disease	+ (ventilated at birth)	+	restrictive lung disease, temporary tracheostomy, and ventilatory support for severe pneumonia at age 3 years	very mild intermittent reactive airway disease, obstructive sleep apnea requiring T & A, CPAP	NA
Short hands/feet	+	+	+	+	+	+	+	+	+
Soft and/or doughy skin	+	+	–	ND	ND	+	–	–	NA
Psychomotor development	normal at 8.5 years	mild motor delay	mild motor delay, walked at 18 months	wheelchair dependent, normal intelligence	NA	+	motor delay	very mild motor delay	NA
Hypophosphatemia	+	–	unknown	+	ND	+	+ resolved age 9 years	+ resolved age 14 years	NA
Renal phosphate wasting	+	–	unknown	+	ND	+	+	+	NA
DEXA scan results	prepamidronate whole body at 4 years 0.419, lastly at 8.5 years 0.58	right distal femur at 6 months 0.289, at 3 years 0.672 (pamidronate × 2 years)	ND	osteopenia	ND	ND	age 17 yr. L2-L4 T score 0.852 g/cm^2	ND	NA
Stature z scores	−9.5	−4.8	ND	ND	ND	ND	−3.5 SD	ND	ND
Other clinical features	dilated cardiomyopathy, hypoplastic right kidney, left bronchial narrowing, history of oral aversion requiring GT feeds	ASD, asthma, left main stem bronchomalacia, dysphagia/aspiration requiring GT feeds	inguinal hernia repair, facial asymmetry, high arched palate	ND	died of respiratory insufficiency at 1 week of age after being taken off ventilator	posterior cleft palate, micrognathia, recurrent aspiration pneumonia, difficulty swallowing requiring NG tube, partial renal tubular acidosis, tracheomalacia	small, narrow thorax, mild elbow and knee flexion contractures, hyperopia, mild systolic hypertension	mild elbow flexion contractures, mild bilateral low-frequency conductive hearing loss	ND

Table 1. *Continued*

Case identifier	AII-1	AII-2	BII-1	CII-1	DII-1	EII-1	FII-1	FII-2	GII-2
Radiographic Findings									
Short long bones	+	+	+	+	+	+	+	+	+
Metaphyseal irregularity and/or cupping	+	+	+	+	+	+	+	+	+
Bony undermineralization	+	+	ND	ND	ND	+	+	+	+
Fractures	+	–	–	–	–	+	+ (ribs age 3 year, complication of hypophosphatemic rickets)	–	–
Angulation of the long bones	+	–	–	+	–	–	+	+	+
Delayed epiphyseal ossification	+	+	+	+	+	+	+	+	NA
Carpal ossification pattern/bone age	3–6 months at 6 years 3 months	newborn at 12 months	newborn at 20 months	newborn at 24 months	ND	no ossification at 3 years	15 years at 16 years 6 months	5 years 6 months at 9 years 6 months	NA
Short and square metacarpals and phalanges	+	+	+	+	+	+	+	+	+
Other radiographic features	ND	calcaneal spurs	calcaneal spurs, odontoid hypoplasia	calcaneal spurs	ND	small, irregular middle phalanges with tapering and periosteal retraction	platyspondyly, small foramen magnum, cervical spinal canal stenosis from skull base to C4, hypoplastic square iliac wings and pubic bones, coxa vara, broad femoral heads, acetabular dysplasia (upsloping of lateral acetabuli)	platyspondyly, small foramen magnum, odontoid hypoplasia, cervical spinal canal stenosis from skull base to C3, hypoplastic square iliac wings, coxa vara	small and flat vertebral bodies, lumbar kyphosis, narrow chest, small and cupped pubic bones

Plus sign (+) indicates presence of a finding, minus sign (–) indicates absence of a finding. Abbreviations: ND, no data available; NA, not applicable, GERP, Genomic Evolutionary Rate Profiling; Birth OFC, birth occipital-frontal circumference; EGA, estimated gestational age; T & A, tonsillectomy and adenoidectomy; CPAP, continuous positive airway pressure; GT, gastrostomy tube; NG, nasogastric.

Figure 1. Characteristic Physical Findings in Children and Adults with Opsismodysplasia

(A–D) Typical features of the face include relative macrocephaly, a prominent forehead, and a short nose with a depressed nasal bridge.

(E and F) Acquired abnormalities resulting from undermineralization of the long bones include bowing of the upper limb (E) and/or lower limb (F).

Case identifiers: AII-1 (A, E, F), AII-2 (B), FII-1 (C), and FII-2 (D), corresponding to those in Table 1, where a detailed description of each individual is provided.

flow-cell loading, the library concentration was determined by triplicate qPCR (Kapa Illumina Library Quantification kit) and molecular weight distributions verified on the Agilent Bioanalyzer. Massively parallel sequencing-by-synthesis via fluorescently labeled, reversibly terminating nucleotides was carried out on the HiSeq sequencer. Samples were sequenced to at least 30× average depth with paired-end 100 bp reads; a third read sequenced the 8 bp index to confirm sample assignments.

Demultiplexed BAM files were aligned to a human reference (hg19) with the Burrows-Wheeler Aligner.[7]

Read data from a flow-cell lane were treated independently for alignment and QC purposes in instances where the merging of data from multiple lanes was required. All aligned read data were subjected to (1) removal of duplicate reads, (2) indel realignment by the GATK IndelRealigner, and (3) base qualities recalibration via GATK TableRecalibration. Variant detection and genotyping were performed with the UnifiedGenotyper (UG) tool from GATK (refv1.529). Variant data for each sample were formatted (variant call format [VCF]) as "raw" calls that contained individual genotype data for one or multiple samples and flagged with the filtration walker (GATK) to mark sites that were of lower quality and potential false positives (e.g., quality scores [≤ 50], allelic imbalance [≥ 0.75], long homopolymer runs [>3], and/or low quality by depth [QD < 5]).
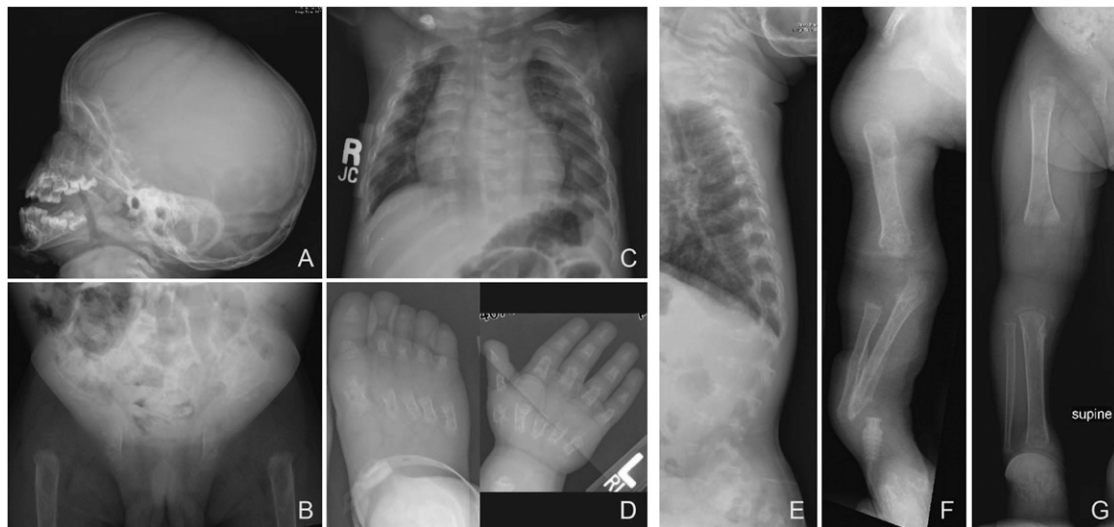
Figure 2. Radiographs of Individual AII-1 at 2 Years and 11 Months of Age

(A) Lateral image of skull showing midface hypoplasia and underdevelopment of the maxilla.

(B) Anterior-posterior (AP) image of the pelvis showing decreased mineralization, dislocated hips, poorly formed acetabula, and loss of normal architecture of the proximal femurs.

(C and E) AP image of the chest notable for under mineralization of the vertebrae and platyspondyly.

(D) The metacarus, metatarsus, and all of the phalanges are short and irregular with flared metaphyses.

(F and G) Delayed mineralization and absence of growth centers in the upper (F) and lower (G) limbs.
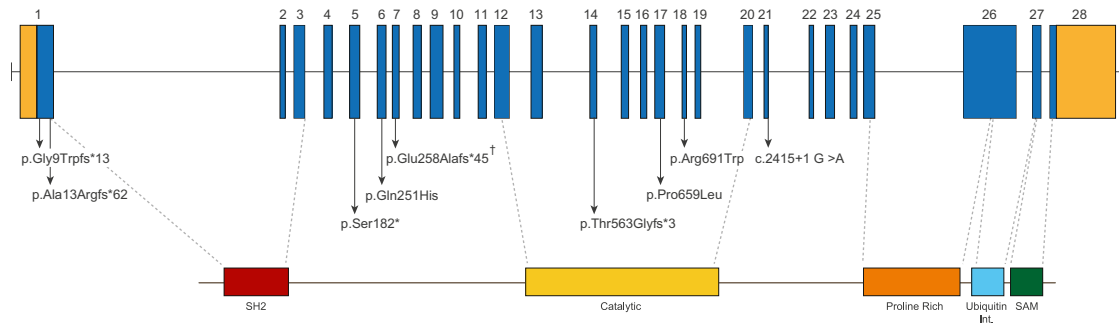
Figure 3. Genomic Structure and Allelic Spectrum of *INPPL1* Mutations that Cause Opsismodysplasia
INPPL1 is composed of 28 exons that encode untranslated regions (orange) and protein coding sequence (blue) domains including SH2 (red), catalytic (yellow), a proline-rich region (orange), ubiquitin-interacting region (light blue), and SAM (green). Arrows indicate the locations of nine different mutations found in seven families with opsismodysplasia. Inverted hatch mark indicates recurrent mutation.

Variant data were annotated with the SeattleSeq Annotation Server.

Regions under linkage peaks covering a total of ~157 Mb were examined for rare and/or novel functional variation including missense, nonsense, splice site mutations, and indels. In the proband (AII-1), novel, homozygous missense mutations for which both parents were heterozygous were identified in five genes (*INPPL1* [MIM 600829], *VPS13A* [MIM 605978], *PRKDC* [MIM 600899], *NEU3* [MIM 604617], and *CARNS1* [MIM 613368]; RefSeq NM_001567.3). Sanger sequencing of these variants in the affected sister of the proband (AII-2) revealed that she was homozygous only for variants in *INPPL1*, *NEU3*, and *CARNS1*, thus reducing the number of candidate genes to three. These candidates were further prioritized based on their putative biological function and screened via Sanger sequencing in an unrelated family with a single child with opsismodysplasia. In the first gene screened, *INPPL1*, the affected child (EII-1 in Table 1), who was the product of a consanguineous mating, was found to be homozygous for a nonsense mutation (c.545C>A [p.Ser182*]).

To determine the extent to which *INPPL1* mutations explain cases of opsismodysplasia, we used Sanger sequencing to screen ten additional unrelated families (total of ten affected individuals and the unaffected parents of a deceased child from whom a DNA sample was unavailable). These families consisted of nine trios in which an affected child was born to unaffected parents and one additional family with two affected siblings. Collectively, between the two families used for discovery and our validation studies, *INPPL1* mutations were found in 7/12 (58%) kindreds tested (Table 1), including both families with more than one individual affected and 5/10 (50%) of the simplex cases. In each of the five families for which DNA was available from one or both parents, heterozygosity for the *INPPL1* mutation was found. No other genes that cause phenotypes similar to opsismodysplasia were tested in the *INPPL1* mutation-negative cases.

A total of nine unique mutations were identified including four frameshift, one nonsense, one splicing, and three missense mutations (Table 1; Figure 3). None of the *INPPL1* missense, nonsense, or splice site mutations identified in the subjects were found in >13,000 chromosomes sequenced as part of the NHLBI-ESP. In three families, the affected individual(s) was a compound heterozygote. In four kindreds, including all three consanguineous families and one family that was not known to be consanguineous, the affected individuals were homozygous for an *INPPL1* mutation. In the latter family (family B in Figure S1), inheritance of the mutation from the mother was confirmed, but the paternal sample was unavailable for testing. It is possible that the father is also a heterozygous carrier of this mutation, but a deletion encompassing the region could not be ruled out. However, this mutation (c.768_769del [p.Glu258Alafs*45]) was also shared in a second unrelated family (family C in Figure S1) of European ancestry, indicating that there may be a carrier population with this variant.

Three of the frameshift mutations and the nonsense mutation are predicted to lead to premature termination codons at the 5′ end of the transcript, suggesting that they lead to loss of INPPL1 function. In particular, homozygosity for the Ser182* mutation found in the index case would eliminate most of the functional domains of the protein, including the catalytic domain (Figure 3). Thus, even if transcripts containing this mutation were stable to nonsense-mediated decay, the resulting truncated protein would be unlikely to retain significant function.

INPPL1 encodes inositol polyphosphate phosphatase-like 1 or SHIP2, a secondary messenger that has multiple roles in developmental processes including cellular proliferation, adhesion, and migration and metabolic functions such as glucose homeostasis and insulin signaling.[8–10] Because of the role of SHIP2 in energy metabolism, it has been intensely studied both in vitro and in animal models. In mice, absence of SHIP2 protein or decreased expression of a catalytically inactive SHIP2 results in multiple developmental defects including a shortened facial profile and diminished growth.[9,10] Specifically, the *Inppl1*^{−/−} mice are about half the size of *Inppl1*^{+/+} mice, suggesting that the axial and appendicular skeleton must be affected.[10]

Inppl1 has been shown to be expressed at E14.5 in the developing axial and appendicular skeletal elements (Eurexpress), further supporting its role in skeletogenesis. The mechanism by which loss of SHIP2 affects skeletal development is unknown because, beyond its catalytic function, SHIP2 has been shown to act as a docking protein for many other cytoplasmic molecules.[11]

In summary, we used linkage analysis and whole-genome sequencing of a consanguineous trio to discover that mutations in *INPPL1* cause opsismodysplasia and explain ~60% of cases in our cohort. The clinical characteristics of individuals with opsismodysplasia caused by *INPPL1* mutations were indistinguishable from those without *INPPL1* mutations and included both individuals with severe renal phosphate wasting and those in whom no such abnormality had been reported. This observation suggests that opsismodysplasia is genetically heterogeneous. Our findings further support a role for SHIP2 in the development of the craniofacial, axial, and appendicular skeleton.[10]

Supplemental Data

Supplemental Data include three figures and can be found with this article online at http://www.cell.com/AJHG/.

Web Resources

The URLs for data presented herein are as follows:

Eurexpress, http://www.eurexpress.org/ee/
FASTX-Toolkit, http://hannonlab.cshl.edu/fastx_toolkit/
GATK, http://www.broadinstitute.org/gatk/
HumanCytoSNP-12 DNA Analysis BeadChip, http://www.illumina.com/products/humancytosnp_12_dna_analysis_beadchip_kits.ilmn
Human Genome Variation Society, http://www.hgvs.org/mutnomen/
NHLBI Exome Variant Server/Sequencing Project (ESP), http://evs.gs.washington.edu/EVS/
Online Mendelian Inheritance in Man (OMIM), http://www.omim.org/
Picard, http://picard.sourceforge.net/
RefSeq, http://www.ncbi.nlm.nih.gov/RefSeq
SAMtools, http://samtools.sourceforge.net/
SeattleSeq Annotation 137, http://snp.gs.washington.edu/SeattleSeqAnnotation137/

References

1. Zonana, J., Rimoin, D.L., Lachman, R.S., and Cohen, A.H. (1977). A unique chondrodysplasia secondary to a defect in chondroosseous transformation. Birth Defects Orig. Artic. Ser. *13* (3D), 155–163.

2. Maroteaux, P., Stanescu, V., Stanescu, R., Le Marec, B., Moraine, C., and Lejarraga, H. (1984). Opsismodysplasia: a new type of chondrodysplasia with predominant involvement of the bones of the hand and the vertebrae. Am. J. Med. Genet. *19*, 171–182.

3. Cormier-Daire, V., Delezoide, A.L., Philip, N., Marcorelles, P., Casas, K., Hillion, Y., Faivre, L., Rimoin, D.L., Munnich, A., Maroteaux, P., and Le Merrer, M. (2003). Clinical, radiological, and chondro-osseous findings in opsismodysplasia: survey of a series of 12 unreported cases. J. Med. Genet. *40*, 195–200.

4. Beemer, F.A., and Kozlowski, K.S. (1994). Additional case of opsismodysplasia supporting autosomal recessive inheritance. Am. J. Med. Genet. *49*, 344–347.

5. Santos, H.G., and Saraiva, J.M. (1995). Opsismodysplasia: another case and literature review. Clin. Dysmorphol. *4*, 222–226.

6. Tyler, K., Sarioglu, N., and Kunze, J. (1999). Five familial cases of opsismodysplasia substantiate the hypothesis of autosomal recessive inheritance. Am. J. Med. Genet. *83*, 47–52.

7. Li, H., and Durbin, R. (2009). Fast and accurate short read alignment with Burrows-Wheeler transform. Bioinformatics *25*, 1754–1760.

8. Clément, S., Krause, U., Desmedt, F., Tanti, J.F., Behrends, J., Pesesse, X., Sasaki, T., Penninger, J., Doherty, M., Malaisse, W., et al. (2001). The lipid phosphatase SHIP2 controls insulin sensitivity. Nature *409*, 92–97.

9. Dubois, E., Jacoby, M., Blockmans, M., Pernot, E., Schiffmann, S.N., Foukas, L.C., Henquin, J.C., Vanhaesebroeck, B., Erneux, C., and Schurmans, S. (2012). Developmental defects and rescue from glucose intolerance of a catalytically-inactive novel Ship2 mutant mouse. Cell. Signal. *24*, 1971–1980.

10. Sleeman, M.W., Wortley, K.E., Lai, K.M., Gowen, L.C., Kintner, J., Kline, W.O., Garcia, K., Stitt, T.N., Yancopoulos, G.D., Wiegand, S.J., and Glass, D.J. (2005). Absence of the lipid phosphatase SHIP2 confers resistance to dietary obesity. Nat. Med. *11*, 199–205.

11. Erneux, C., Edimo, W.E., Deneubourg, L., and Pirson, I. (2011). SHIP2 multiple functions: a balance between a negative control of PtdIns(3,4,5)P$_3$ level, a positive control of PtdIns(3,4)P$_2$ production, and intrinsic docking properties. J. Cell. Biochem. *112*, 2203–2209.